Pulse Position-Based Spatial Modulation for Molecular Communications

Mustafa Can Gursoy, *Student Member, IEEE,* Ertugrul Basar, *Senior Member, IEEE,* Ali Emre Pusane, *Member, IEEE,* and Tuna Tugcu, *Member, IEEE*

***Abstract*—Multiple-input-multiple-output (MIMO) approaches have been recently introduced to molecular communications (MC) in order to increase the communication throughput. For MIMO systems, index modulation (IM) suggests encoding information bits using the indices of the available antennas, rather than employing spatial multiplexing or performing other space-time coding schemes. Recent works have shown that utilizing the available MIMO antennas with IM-based approaches improves the error performance of a molecular MIMO system, courtesy of molecular-IM's robustness against inter-symbol interference and inter-link interference (ILI). Inspired by IM's prospects on MC, this letter proposes a novel family of IM-based schemes to the MC realm. The proposed schemes combine position-based constellations with antenna indices to encode bits in and yield reliable error performances due to their robustness against ILI.**

***Index Terms*—Molecular communications, molecular MIMO, spatial modulation, pulse position modulation, index modulation.**

I. Introduction

Molecular communications (MC) is a novel communications paradigm that uses chemical signals to convey information. In an MC system, information can be encoded in the quantity, type, time of release, and combinations of these physical quantities of the messenger molecules (MMs) [1]. In diffusion-based molecular communications (DBMC), the MMs propagate through the communication environment according to the rules of Brownian motion, which introduces inter-symbol interference (ISI) into the DMBC channel and hinders communicating at high data rates.

As demonstrated by several works, including but not limited to [2]–[4], multiple-input-multiple-output (MIMO) transmission can be used in MC systems to enhance communication performance. Furthermore, [5] introduces the index modulation (IM) concept ([6]) to the MC realm, and proposes single and dual-molecule IM-based schemes to the MC literature. As a single-molecule scheme, [5] proposes molecular space shift keying (MSSK) in which the information is encoded solely in the antenna index. In the same study, the use of two types of MMs is also considered by proposing quadrature molecular space shift keying (QMSSK) and molecular spatial modulation (MSM). QMSSK transmits two MSSK symbols in parallel, whilst MSM combines binary molecule shift keying constellations as a complement to the space constellations.

In addition, [7] combines the antenna index symbols with concentration shift keying (CSK) constellations and provides a way of performing spatial modulation for MC, using a single MM type. One challenge with using CSK constellations for molecular-IM schemes is that in order to decode CSK constellations better, the constellation points need to be further apart from each other. On the other hand, if a CSK constellation point is chosen close to zero in order to create the desired distance between CSK constellation points, determining the activated antenna becomes very difficult.

As originally proposed by [8] to the MC realm, pulse position modulation (PPM) encodes bits in the temporal position of the transmitted molecular pulse. Inspired by the promising results of [9] for higher order single-input-single-output (SISO) PPM schemes on DBMC systems, main contribution of this letter is the introduction of the scheme of molecular position-SM (MPSM) to molecular communications. Our proposed family of molecular-IMs encode symbols using PPM constellations, accompanied by the symbols using the antenna indices, extending the works of [5] and [7].

One advantage of the proposed schemes is that they always emit a constant number of MMs to the channel for each symbol due to the very nature of PPM, unlike existing CSK-based molecular-IM approaches. This property helps the receiver to identify the activated antenna easier by avoiding constellations with small numbers of transmitted MMs, which is otherwise an issue for CSK-based IM schemes. In addition, the receiver utilizes a detection method called the joint maximum count decoder (JMCD) in the letter, to jointly decode the constellation and antenna index symbols. JMCD performs a simple $\arg\max$ operation among the received molecule counts, and does not require the channel impulse response (CIR) at the receiver end. This property is an advantage over CSK-based IM schemes, since they require CIR for thresholding or distance-calculating when decoding the CSK-encoded symbols. Since this work considers a MIMO setting similar to [2]–[5], [7], it requires a higher device complexity to realize and is more suitable for synthetic MC systems. Overall, the main contribution of this paper can be thought of allocating this available complexity more efficiently that existing approaches in the literature.

II. System Model

The system model considered in this letter is adopted from the channel model in [5]. The overall system includes a communication scenario between a single transmitter (TX) unit and a single synchronized receiver (RX) unit in an unbounded, 3-D, driftless diffusion environment, using MMs with diffusion coefficient D. The TX unit is equipped with n_{Tx} point sources that can emit molecules and act as *transmit antennas*. Similarly, the RX unit has n_{Rx} spherical absorbing receivers, each with radius r_r, that act as *receiver antennas*. For this letter, $n_{Tx} = n_{Rx} = 4$ is chosen for demonstrative

M. C. Gursoy, A. E. Pusane, and T. Tugcu are with Bogazici University, Istanbul, Turkey. e-mail: {can.gursoy, ali.pusane, tugcu}@boun.edu.tr

E. Basar is with Koç University, Istanbul, Turkey. e-mail: ebasar@ku.edu.tr

This article has been accepted for publication in a future issue of this journal, but has not been fully edited. Content may change prior to final publication. Citation information: DOI 10.1109/LCOMM.2019.2898190, IEEE Communications Letters

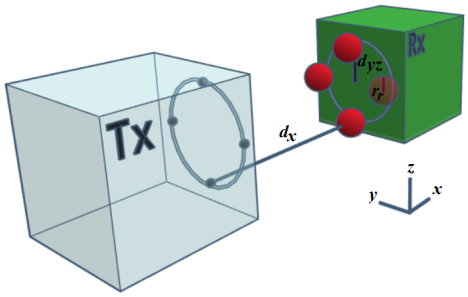

Fig. 1. The system model for $n_{Tx} = n_{Rx} = 4$.

purposes. Similar to [5], the TX body is transparent to the MMs after emission and the RX body is perfectly reflective.

The TX and RX units and their corresponding transmit and receiver antennas are assumed to be perfectly aligned against each other. The distance between the closest point of a receiver spherical antenna and its corresponding transmit point antenna is denoted with d_x. On each unit, the antennas are placed in a uniform circular array (UCA), similar to the system considered in [5], with $\frac{\pi}{2}$ angular separation between them, since $n_{Tx} = n_{Rx} = 4$. The distance between the projection of a spherical receiver antenna on its surface and the center of the RX UCA is denoted as d_{yz}. Note that this notation implies that the radius of the TX UCA is equal to $d_{yz}+r_r$. The overall system model diagram is presented in Fig. 1.

Since the system has multiple absorbing spherical receivers, the arrivals to each RX antenna become dependent. In such a case, in order to generate the channel coefficients, $h_{i,j}[n]$ ($n = 1, \ldots, L_c$, where L_c is the channel memory), this letter uses random-walk-based Monte Carlo simulations described by [2] and [5]. The expression $h_{i,j}[n]$ represents the n^{th} channel coefficient on the RX antenna with index j when an emission from the i^{th} TX antenna occurs. When transmitting multiple MMs, the number of arriving MMs at the receiver end are approximated as independent binomial distributions with success probabilities $h_{i,j}[n]$ following the approaches of [2], [4], [5], which can be approximated with independent Gaussian random variables (RV) [10]. Denoting the arrival count to the j^{th} receiver antenna at time slot m as $R_j[m]$, we can state $R_j[m] \sim \mathcal{N}(\mu_j[m], \sigma_j^2[m])$, where

$$\mu_j[m] = \sum_{z=m-L_c+1}^{m} \sum_{i=1}^{n_{Tx}} s_i[z] h_{i,j}[m-z+1] \quad (1)$$

and

$$\sigma_j^2[m] = \sum_{z=m-L_c+1}^{m} \sum_{i=1}^{n_{Tx}} s_i[z] h_{i,j}[m-z+1]\big(1-h_{i,j}[m-z+1]\big). \quad (2)$$

Here, m is the discrete time index, and $s_i[m]$ denotes the number of transmitted MMs from the i^{th} TX antenna, at the m^{th} discrete time.

III. Proposed Schemes

In this letter, we introduce a novel SM family to the MC literature. The proposed scheme combines PPM-encoded constellations with the molecular MIMO antenna indices to convey information. In an $n_{Tx} \times n_{Rx}$ molecular MIMO system where $n_{Tx} = n_{Rx} = \beta$, $\log_2 \beta$ bits can be encoded into the antenna index. In addition, the proposed scheme encodes another $\log_2 \alpha$ bits using an α-PPM constellation on top of the $\log_2 \beta$ bits encoded in the antenna index, transmitting a total of $\log_2 \alpha + \log_2 \beta$ bits for each channel use. To generalize this PPM-encoded SM family, we call the scheme (α, β)-molecular position-spatial modulation ((α, β)-MPSM), where α and β denote the order of the utilized PPM and the number of antennas at the TX&RX end, respectively. A demonstrative codebook for $(2, 4)$-MPSM is presented in Table I.

TABLE I
Transmission strategy for $(2, 4)$-MPSM with natural binary mapping on the antenna index

Bit seq.	PPM chips / Antenna Index	$x[k]$	Bit seq.	PPM chips / Antenna Ind.	$x[k]$
0 00	01 / 1	1	1 00	10 / 1	2
0 01	01 / 2	5	1 01	10 / 2	6
0 10	01 / 3	3	1 10	10 / 3	4
0 11	01 / 4	7	1 11	10 / 4	8

In the transmission strategy for (α, β)-MPSM, the data bit stream $\mathbf{u}$ is divided into bit sequences/blocks of length $\log_2 \alpha + \log_2 \beta$, where $\mathbf{u}[k] \in \{0, 1\}$. In each block, the first $\log_2 \alpha$ bits denote the PPM sequence to be transmitted. Throughout the letter, each element of the PPM sequence is referred to as a chip. The said α-chip long PPM sequence is then transmitted from the activated antenna whose index is determined by the last $\log_2 \beta$ bits in the block. For further reference, we define $x[k]$ as the decimal MPSM symbol corresponding to the joint symbols of the k^{th} PPM and the k^{th} activated antenna index, which is equal to

$$x[k] = 1 + \sum_{z=Bk-B+1}^{Bk} 2^{z-(Bk-B+1)} u[z], \quad (3)$$

where $B = (\log_2 \alpha + \log_2 \beta)$. By definition, $x[k] \in \{1, \ldots, \alpha\beta\}$. Also, as initially proposed by [5], Gray coding may also be utilized to map the β-bit strings to the activated molecular MIMO antennas when mapping the $\mathbf{u}$ sequence onto the $x[k]$ sequence, in order to lower the amount of bit errors for ILI-caused symbol errors.

When different MC schemes are to be compared in terms of error performance, the comparison needs to be performed under the same *bit duration* (t_b) and *transmitted molecules per bit* (M) normalizations [5], [9]. The former normalization is done to compare the schemes under equal data rates, and the latter one is to normalize the energy consumption on a per-bit basis. Naturally, schemes that are able to encode more bits in a single channel use are allowed to transmit using more MMs and at a longer symbol duration (t_s) per channel use. To comparatively illustrate the transmitted molecules and the symbol/chip slot durations per channel use, Table II is presented. Since higher order PPM schemes divide the available t_s into more chip slots of length t_c, the increase in t_s due to transmitting more bits per channel use may not translate to an increase in t_c. The chip duration of (α, β)-MPSM can be formulated as $t_c = \frac{(\log_2 \alpha + \log_2 \beta) t_b}{\alpha}$. In Table II, the molecular-IM scheme proposed by [7] which combines the antenna index with BCSK, is termed as BCSK-SM. Note that BCSK-SM is modeled to transmit a BCSK bit-1 by emitting $4M$ molecules,

This article has been accepted for publication in a future issue of this journal, but has not been fully edited. Content may change prior to final publication. Citation information: DOI 10.1109/LCOMM.2019.2898190, IEEE Communications Letters

TABLE II
SLOT DURATIONS AND TRANSMITTED MOLECULES PER SYMBOL VALUES OF THE PROPOSED AND EXISTING MOLECULAR-IM SCHEMES

Modulation Scheme	4-MSSK	4×4 BCSK-SM	$(2,4)$-MPSM	$(4,4)$-MPSM	$(8,4)$-MPSM
Transmitted bits per unit symbol	2	3	3	4	5
Chips per symbol	1	1	2	4	8
Slot duration (t_s for MSSK and BCSK-SM, t_c for MPSM)	$2t_b$	$3t_b$	$\frac{3}{2}t_b$	t_b	$\frac{5}{8}t_b$
Bit duration	t_b	t_b	t_b	t_b	t_b
Molecules per symbol	$2M$	$2M$ for bit-0, $4M$ for bit-1,	$3M$	$4M$	$5M$
Molecules per bit	M	M	M	M	M

and bit-0 with $2M$ molecules, following the description of the scheme [7].

At the receiver end, the synchronized receiver collects molecule arrival counts for all antennas at every chip slot of the corresponding transmission, and finds the maximum among all $\alpha \times \beta$ arrival counts. The decoding operation for (α, β)-MPSM can be denoted as

$$\begin{aligned} < \hat{j}, \hat{m} > = \arg \max_{\substack{j \in \{1,\cdots,\beta\} \\ m \in \{\alpha k - \alpha + 1, \cdots, \alpha k\}}} R_j[m], \\ \hat{\mathcal{J}}[k] = \hat{j}, \;\; \hat{\mathcal{M}}[k] = \hat{m} - (\alpha k - \alpha), \end{aligned} \tag{4}$$

where $\hat{\mathcal{J}}[k]$ and $\hat{\mathcal{M}}[k]$ denote the decoded antenna index and decoded PPM chip index for the k^{th} MPSM symbol, respectively. After obtaining $\hat{\mathcal{J}}[k]$ and $\hat{\mathcal{M}}[k]$, the receiver can re-construct $\hat{x}[k]$ and the corresponding bit sequence $\big[\hat{\mathbf{u}}[Bk-B+1] \quad \cdots \quad \hat{\mathbf{u}}[Bk-1] \quad \hat{\mathbf{u}}[Bk]\big]^T$, according to the encoding mapping. Note that this decoder is memoryless, since it performs the decoding operation by taking a joint maximum among all candidates only for the current joint symbol, $x[k]$. Overall, the decoder can be thought of as a direct extension to the maximum count decoder (MCD) presented in [5], and hence it is named as the joint maximum count decoder (JMCD) in the letter.

A. Error Probability Analysis

Since MC systems have signal-dependent ISI and noise, the error performance is found by evaluating and averaging over all possible symbol sequences in a channel with symbol memory L [5], [10]. Adapting this idea to the MPSM scheme, the theoretical BER of (α, β)-MPSM can be formulated as

$$P_e = \sum\nolimits_{\forall x[k-L+1:k]} \left(\frac{1}{\alpha\beta}\right)^L P_{e|x[k-L+1:k]}, \tag{5}$$

where $x[k-L+1:k]$ denotes the MPSM symbol vector $\big[x[k-L+1] \quad \cdots \quad x[k-1] \quad x[k]\big]^T$. In (5), $P_{e|x[k-L+1:k]}$ is the conditional error probability given the MPSM symbol sequence $x[k-L+1:k]$, and can be expressed by

$$P_{e|x[k-L+1:k]} = \sum\nolimits_{l=1}^{\alpha\beta} \frac{d_H(\mathbf{u}_{x[k]}, \mathbf{u}_l)}{\log_2 \alpha + \log_2 \beta} P(\hat{l}). \tag{6}$$

Here, $P(\hat{l})$ is the probability of decoding the decimal MPSM symbol l given $x[k-L+1:k]$ are transmitted. Thus, $P(\hat{l})$ corresponds to the probability of the arrival count associated with the MPSM symbol l being the largest among all $R_j[m]$ where $j \in \{1, \cdots, \beta\}$ and $m \in \{\alpha k - \alpha + 1, \cdots, \alpha k\}$. Furthermore, $\mathbf{u}_{x[k]}$ and $\mathbf{u}_l$ denote the $\log_2 \alpha + \log_2 \beta$ bits-long sequences that correspond to the MPSM symbols $x[k]$ and l, respectively. $d_H(\cdot)$ finds the Hamming distance (number of differing bits) between its argument vectors. Overall, the summation in (6) calculates the average bit error when l is decoded as the MPSM symbol and multiplies it with the probability of this event's occurence. In other words, (6) can be thought of as the weighted average that yields the error probability, conditioned on $x[k-L+1:k]$. After this point, finding $P(\hat{l})$ for $l \in 1, \cdots, \alpha\beta$, given $x[k-L+1:k]$, is the only expression required to obtain the theoretical BER.

All arrival counts ($R_j[m]$'s) are modeled as independent Gaussian RVs with means and variances obtained by (1) and (2), respectively. Following the similar derivation of [5], the probability of the Gaussian RV with index l being the largest among all $\alpha\beta$ independent Gaussian RVs can be written as

$$P(\hat{l}) = \int_{-\infty}^{\infty} \left[\prod\nolimits_{\substack{\tau=1 \\ \tau \neq l}}^{\alpha\beta} P\big(R_\tau < r\big) \right] f_{R_l}(r) dr, \tag{7}$$

where R_τ and R_l denote the Gaussian RVs associated with the MPSM symbols with indices τ and l, respectively. $f_{R_l}(r)$ denotes the Gaussian probability density function of $R_j[m]$ that is associated to R_l, which can be written as $f_{R_l}(r) = \frac{1}{\sqrt{2\pi\sigma_j^2[m]}} \exp\big(\frac{-(r-\mu_j[m])^2}{2\sigma_j^2[m]}\big)$. Furthermore, $P\big(R_\tau < r\big)$ denotes the probability that R_τ is smaller than a dummy variable r, and is equal to $Q\Big(\frac{\mu_\tau[k]-r}{\sqrt{\sigma_\tau^2[k]}}\Big)$.

After obtaining $P(\hat{l})$, derivation of the theoretical BER expression is concluded by plugging (7) into (6), and then (6) into (5). Note that since calculating (5) requires evaluating over all $x[k-L+1:k]$ sequences, the theoretical BER's numerical computation is computationally very expensive, with complexity on the order of $\mathcal{O}\big((\alpha\beta)^L\big)$.

IV. NUMERICAL RESULTS AND DISCUSSION

This section presents the bit error rate (BER) performances of the proposed schemes, MSSK, BCSK-SM, and their Gray coded variants, using the theoretical BER expression and computer simulations. In the comparisons, MSSK is demodulated using the MCD [5]. BCSK-SM is demodulated using the equal gain combining (EGC) assisted Euclidean distance method as described in Eqs. (27)-(29) of [7]. All results are obtained on the MIMO system model in Fig. 1, which has absorbing RX antennas, rather than using passive receivers considered in [7]. For SISO schemes, a point TX and an absorbing spherical RX are used [9]. SISO BCSK is realized with on-off keying.

The analysis made in Fig. 2 demonstrates that the theoretical BER expressions found in Subsection III-A are in agreement

This article has been accepted for publication in a future issue of this journal, but has not been fully edited. Content may change prior to final publication. Citation information: DOI 10.1109/LCOMM.2019.2898190, IEEE Communications Letters

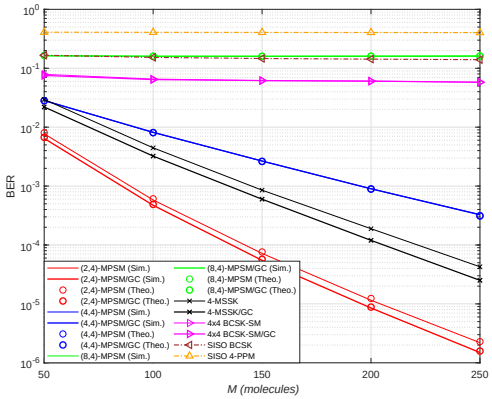

Fig. 2. BER vs. M curves for MIMO and SISO MC schemes. $t_b = 0.3$s, $d_x = 8\mu$m, $d_{yz} = 3\mu$m, $D = 79.4\,\mu m^2/s$, $r_r = 5\mu$m, and $L = 4$. Both natural and Gray coded (GC) variants are included.

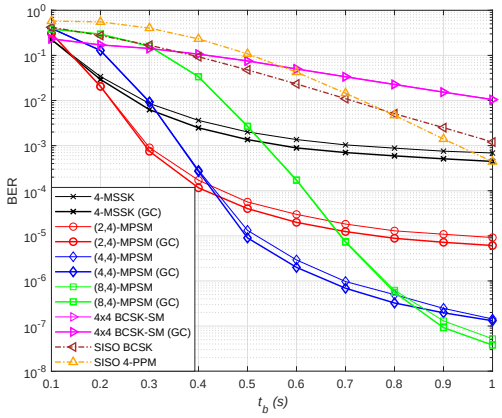

Fig. 3. BER vs. t_b for MIMO and SISO MC schemes. $M = 100$ molecules, $d_x = 8\mu$m, $d_{yz} = 3\mu$m, $D = 79.4\,\mu m^2/s$, $r_r = 5\mu$m, $L = 30$.

with the simulation results. In addition, for the channel parameters for Fig. 2, $(2,4)$-MPSM has a lower BER than 4-MSSK, whilst higher order MPSM schemes perform worse. For further explanation, a BER vs. t_b analysis is presented in Fig. 3.

The results in Fig. 3 show that, while satisfying a certain BER constraint, MPSM provides an increase in the bit rate when compared to the existing approaches. Furthermore, Fig. 3 implies that the data rate increase provided by the proposed schemes is prominent, especially when the BER requirements are lower. For example, $(2,4)$-MPSM can yield a BER of 10^{-3} when communicating at a bit duration of $t_b \simeq 0.29$s for the system in Fig. 3, whilst Gray-coded 4-MSSK can satisfy the same BER constraint for $t_b \simeq 0.56$s. Note that these results correspond to roughly a two-fold increase in the data rate while conserving the reliability of the communication. This phenomenon is mainly due to the ILI-caused error floor associated with MSSK and BCSK-SM. As also pointed out in [5], increasing t_b helps to reduce ISI greatly, but waiting for longer symbol durations at the receiver end also causes the arrivals to the receiver antennas to become more uniform, causing ILI. This effect is mitigated in MPSM, since the chip durations of PPM are still short enough, even for larger t_b.

On the other hand, short chip durations are more prone to ISI, which becomes an issue when communicating at very low bit durations. When t_b is already very small, MPSM further divides the symbol interval into PPM's even shorter chip slots, which increases ISI. This explains the worse performance of the MPSM schemes at $t_b = 0.1$s when ISI is extremely high. MPSM schemes with higher order PPM constellations suffer more from this effect. This adverse effect explains the trend in Fig. 2 and that higher order PPMs require a longer t_b to overcome ISI and surpass existing schemes due to their better ILI combating in Fig. 3. Overall, it can be inferred from Fig. 3 that MPSM schemes provide a good trade-off between ISI and ILI combating, and surpass existing molecular SM schemes in terms of the bit rate while satisfying a reliable BER constraint.

Even though figures are not provided here, our results confirm that relative performances of the schemes follow the same trend for different d_x and r_r values. However, error rates of all molecular-IM schemes increase with d_x, due to MMs taking longer times to reach the RX and arriving more uniformly among antennas. This limits the range of molecular-IM schemes in general, since increasing d_x makes it more difficult for the RX to determine the activated TX antenna.

V. Conclusion

In this letter, we have introduced novel molecular-IM schemes that employ PPM symbols as constellations. We have shown that the proposed schemes outperform existing molecular-IM schemes in terms of ILI combating and provide higher data rates while maintaining a low error probability.

References

[1] N. Farsad *et al.*, "A comprehensive survey of recent advancements in molecular communication," *IEEE Commun. Surveys Tuts.*, vol. 18, no. 3, pp. 1887–1919, Feb. 2016.
[2] B. H. Koo *et al.*, "Molecular MIMO: From theory to prototype," *IEEE J. Sel. Areas Commun.*, vol. 34, no. 3, pp. 600–614, Mar. 2016.
[3] L. S. M. *et al.*, "MIMO communications based on molecular diffusion," in *Proc. IEEE GLOBECOM*, Dec. 2012, pp. 5380–5385.
[4] M. Damrath, H. B. Yilmaz, C. Chae, and P. A. Hoeher, "Array gain analysis in molecular MIMO communications," *IEEE Access*, vol. 6, pp. 61 091–61 102, Oct. 2018.
[5] M. C. Gursoy, E. Basar, A. E. Pusane, and T. Tugcu, "Index modulation for molecular communication via diffusion systems," *IEEE Trans. Commun.*, to appear, Feb. 2019.
[6] E. Basar *et al.*, "Index modulation techniques for next-generation wireless networks," *IEEE Access*, vol. 5, pp. 16 693–16 746, Aug. 2017.
[7] Y. Huang *et al.*, "Spatial modulation for molecular communication," *arXiv preprint arXiv:1807.01468*, July 2018.
[8] N. Garralda *et al.*, "Diffusion-based physical channel identification in molecular nanonetworks," *Nano Commun. Netw.*, vol. 2, no. 4, pp. 196–204, Dec. 2011.
[9] B. C. Akdeniz, A. E. Pusane, and T. Tugcu, "Position-based modulation in molecular communications," *Nano Commun. Netw.*, vol. 16, pp. 60–68, June 2018.
[10] H. B. Yilmaz, C.-B. Chae, B. Tepekule, and A. E. Pusane, "Arrival modeling and error analysis for molecular communication via diffusion with drift," in *Proc. ACM NANOCOM*, Sep. 2015.